

VIII- II -1. Project Research

Project 9

Q. Xu

Research Reactor Institute, Kyoto University

OBJECTIVES: In addition of neutron irradiations, ion and electron irradiations are widely used to estimate degradation mechanical properties of materials and develop new materials, such as material for optoelectronic and high-power devices. In the present report, majority results of project research were obtained by ion, electron and γ ray irradiations because operation time of KUR was limit in 2013.

RESULTS: Defects induced by the irradiation influence the electrical and mechanical properties of semiconductor and metals. They also change the element distribution in alloys. Gas atoms, such as hydrogen, are trapped by the vacancies, and hydrogen-vacancy complexes degrade the mechanical property of metals. The allotted research subject (ARS) and the name of co-researches in each ARS are listed below. Details are presented in this progress reports.

ARS-1

Nitrogen interstitial defect as a compensation center in neutron transmutation doped GaN. (K. Kuriyama et al.)

ARS-2

Neutron irradiation effects of superconducting magnet materials at low temperature. (T. Nakamoto et al.)

ARS-3

Study on fine structures formed by high energy particle irradiation. (A. Kinomura et al.)

ARS-4

Thermo- and photo-luminescence of pink calcite. (T. Awata et al.)

ARS-5

A new indirect water-cooling electron-irradiation system for LINAC. (M. Akiyoshi et al.)

ARS-6

The development of KUR positron beam system and age-momentum correlation apparatus. (Y. Nagai et al.)

ARS-7

Radiation damage in bulk amorphous alloys by electron irradiation. (F. Hori et al.)

ARS-8

Positron annihilation study on Fe-40Cr alloy after electron irradiation. (T. Onitsuka et al.)

ARS-9

Damage evolution in neutron-irradiated metals during neutron irradiation at elevated temperatures. (I. Mukouda, et al.)

ARS-10

Irradiation hardening of Fe-Cr alloy after neutron irradiation in KUR. (R. Kasada et al.)

ARS-11

Hydrogen trapping sites at grain boundaries in neutron-irradiated nanocrystalline Ni. (H. Tsuchida et al.)

ARS-12

Positron annihilation spectroscopy in D₂ implanted tungsten. (K. Sato et al.)

ARS-13

Effects of high energy particle irradiation on hydrogen retention in refractory metals. (K. Tokunaga et al.)

ARS-14

Fabrication of Josephson junction utilizing nanocell on compound semiconductor GaSb. (K. Shigematsu et al.)

ARS-15

Trapping of hydrogen isotopes in radiation defects in Tungsten. (Y. Hatano et al.)

CONCLUSIONS: Radiation effects were investigated in solid materials, such as semiconductor, metals. In addition, the interaction between gas atom and defects were also studied. It is clear that defects produced by the irradiation are the key factor to change the electrical and mechanical properties of solid materials.

K. Kuriyama, K. Kamioka, T. Nakamura, K. Kushida¹
and Q. Xu²

College of Engineering and Research Center of Ion
Beam Technology, Hosei University

¹Osaka Kyoiku University

²Research Reactor Institute, Kyoto University

INTRODUCTION: The 1000 °C annealed neutron transmutation doped (NTD)-GaN keeps having high resistivity of $10^8 \Omega\text{cm}$ at room temperature. In the present study, we report the origin of high resistivity by combining an alternating current (ac) Hall effect and the Rutherford backscattering spectroscopy (RBS)/channeling measurements.

EXPERIMENTS: GaN epitaxial films on sapphire substrates were irradiated with fast and thermal neutrons at fluences of $6.7 \times 10^{18} \text{ cm}^{-2}$ and $1.4 \times 10^{19} \text{ cm}^{-2}$, respectively. We carried out an ac-Hall effect measurement and clarified the existence of deep energy level from the temperature dependence of carrier concentration in high temperature region. To clarify the lattice displacement related to the deep level, RBS/channeling measurements were performed using the Van de Graaff accelerator of Hosei University.

RESULTS: Figure 1 shows the temperature dependence of carrier concentration at 150 - 400 °C for the 1000 °C annealed samples. All annealed samples showed the n-type conduction. The solid line represents the linear approximation. The activation energy estimated from the slope of the linear approximation was 960 meV. The energy is consistent with the theoretical value of N interstitial (N_i) [2].

Figures 2 (a) and (b) show typical random and aligned RBS spectra of as-irradiated and 1000 °C annealed GaN, respectively. The values of minimum yield χ_{min} for N were 12.2 % for un-irradiated, 34.4 % for as-irradiated, and 21.8 % for 1000 °C annealed samples. The displacement concentration of N atoms estimated from the values of χ_{min} for N is $4.5 \times 10^{21} \text{ cm}^{-3}$, which is about two orders of magnitude higher than that of Ga atoms. Neutron-transmuted DX-like center of Ge as a donor [1] would be compensated by both N_i as deep acceptors and ^{14}C acceptors [3] generated from a (n,p) reaction of ^{14}N . The origins of high resistivity are attributed to these acceptors.

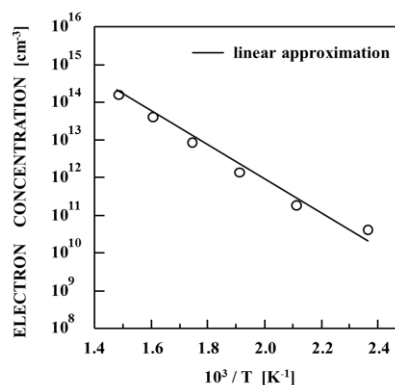


Fig 1. The temperature dependence of carrier concentration for 1000 °C annealed NTD-GaN.

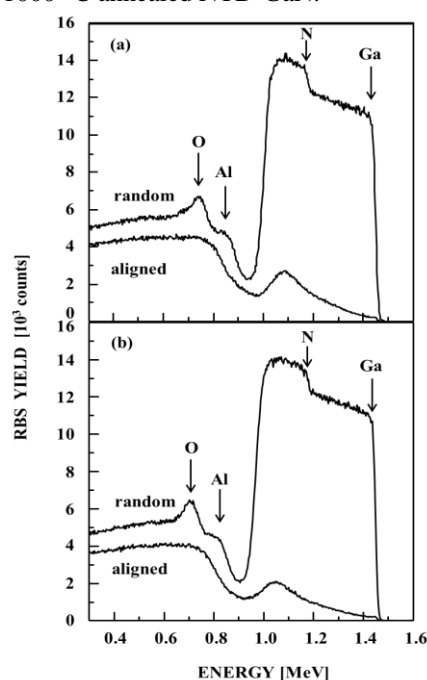


Fig 2. Aligned and random RBS spectra for (a) as-irradiated and (b) 1000 °C annealed NTD-GaN using 1.5-MeV H^+ ions.

The authors would like to thank Dr. M. Hasegawa of AIST for the ac-Hall effect measurements.

REFERENCES:

- [1] K. Kuriyama, T. Tokumasu, Jun Takahashi, H. Kondo, and M. Okada, Appl. Phys. Lett. **80**, 3328 (2002); Proceedings of 26th Int. Conf. Physics of Semiconductors (Edinburgh, UK) D46 (2002).
- [2] J. Neugebauer and C. G. Van de Walle, Phys. Rev. B **50**, 8067 (1994).
- [3] T. Ida, T. Oga, K. Kuriyama, K. Kushida, Q. Xu, and S. Fukutani, AIP Conference Proceedings, **1566**, 67 (2013) (31st Int. Conf. Physics of Semiconductors, Zurich, Switzerland, 2012).

T. Nakamoto, M. Yoshida, T. Ogitsu, Y. Makida,
K. Sasaki, S. Mihara, K. Yoshimura, H. Nishiguchi,
M. Sugano, M. Iio, Y. Kuno¹, M. Aoki¹, A. Sato¹, Q. Xu²,
K. Sato², Y. Kuriyama² and Y. Mori²

J-PARC Center, KEK

¹*Department of Physics, Osaka University*

²*Research Reactor Institute, Kyoto University*

INTRODUCTION: The superconducting magnets will be subjected to a high neutron fluence of 10^{21} n/m² or higher in the operation lifetime in the high energy particle physics experiments, such as a high luminosity upgrade of the LHC at CERN and the muon source for the COMET experiment at J-PARC. Since electrical resistivity of a stabilizer at low temperature, which is very sensitive to neutron irradiation, is one of the important parameters for the quench protection of the magnet system. A series of electrical resistivity measurement at neutron irradiation for the aluminum stabilizer with additives of yttrium taken from the prototype superconducting cable as well as copper stabilizer was started in 2011. In 2013, the third irradiation test with the same samples in 2011 and 2012 was performed to observe the effect of the multiple irradiations and the thermal cycles to room temperature. In addition, irradiation on a new aluminum stabilizer sample with nickel additive taken from the real conductor was started.

EXPERIMENTS: The irradiation tests have been carried out at a low temperature irradiation facility (LTL) at E-4 line of KUR. The aluminum stabilizer samples (RRR of 360 for Y additive and 560 for Ni additive) with dimensions of 1 mm x 1 mm x 70 mm were cut from the superconducting cable manufactured by Hitachi Cable. The copper stabilizer sample (RRR of 300) also has the same dimensions. The electric resistance was measured by a 4-wire method employing a Keithley 6221 current source and a Keithley 2182A voltmeter. The temperature was determined by using a thermocouple of Au(Fe) and Chromel, since the Cernox sensor (CX-1050-SD) showed a temperature drift during neutron exposure due to the irradiation damage. The thermocouple and the Cernox sensor were placed just behind the samples to measure the temperature of the helium gas coolant.

RESULTS: The third irradiation test for the aluminum sample (Al-Y2) and the copper sample was carried out in July 2013. The new aluminum sample with Ni additive (Al-Ni) was irradiated at first time. The irradiation condition is basically same as the first and the second irradiation in 2011 and 2012. After cooling down to 13 K, the reactor was turned on to a power of 1 MW. The estimated

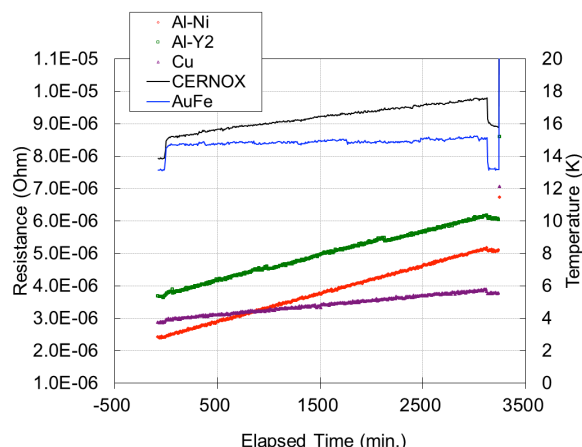


Fig. 1. Electrical resistance of aluminum and copper stabilizer samples during the neutron irradiation in 2013.

fast neutron fluence in 52 hours operation is 2.6×10^{20} n/m². Resistance of the samples and temperature variations during the irradiation are shown in Fig. 1. The temperature jumped from 13 K to 15 K at the beginning due to radiation from the reactor core. During exposure the thermocouple indicates stable temperature while the Cernox sensor readout drifts up to 18 K due to irradiation damage. Behavior of the induced resistance by the neutron irradiation is very similar to the previous results in 2011 and in 2012: the resistances of Al-Y2 and copper show linear increase with respect to the neutron fluence during the exposure. Degradation rates of the electrical resistivity at the fluence of 10^{20} n/m² for both aluminum samples are quite similar: 2.5×10^1 pΩm and 2.3×10^1 pΩm for Al-Y2 and Al-Ni, respectively. For copper sample, the degradation rate is 7.7 pΩm at the fluence of 10^{20} n/m² while the previous rate in 2012 was 10.2 pΩm.

Anneal effects of the samples due to the thermal cycle to room temperature were observed. For the aluminum samples, the induced resistance was fully recovered to be the original resistance as seen in the previous cycles. For the copper sample, however, the recovery of the resistance by the thermal cycle was imperfect, as observed in the previous cycles. The recovery rates, defined as how much induced electrical resistivity due to the irradiation is recovered by the thermal cycle, were 82 % and 92 % for the first and the second irradiations, respectively. Further recovery behavior of the copper sample should be checked at the next cooling in 2014.

PR9-3 Study on Fine Structures Formed by High Energy Particle Irradiation

A. Kinomura, K. Sato¹, Q. Xu¹ and T. Yoshiie¹

National Institute of Advanced Industrial Science and Technology (AIST)

¹Research Reactor Institute, Kyoto University

INTRODUCTION: Irradiation effects of ion irradiation have been extensively studied for various crystalline materials. In general, irradiation damage degrades crystallinity and gives harmful effects on material properties. However, under appropriate irradiation conditions, the irradiation effects can induce interesting phenomena. A typical example of such effects is the ion beam annealing in Si, where implantation-induced damage layers are recovered by other ion irradiation. Thus, it is important to investigate the irradiation effects of energetic particles (ions and neutrons) and the influence on material structures.

EXPERIMENTS: Neutron enhanced annealing (crystalline recovery) of ion-implantation induced damage in single-crystalline Si was investigated. Si ion implantation to single crystalline Si was performed at 200 keV to a dose of $5 \times 10^{14} \text{ cm}^{-2}$ to introduce radiation damage. The Si-implanted sample was encapsulated in an Al capsule with He ambient gas and neutron irradiated for 12 weeks in the core irradiation facility of the Kyoto University Reactor (KUR) operating at 5 MW. Control samples were thermally annealed at 90 °C in a quartz tube furnace with flowing Ar gas for the same period as the neutron irradiation. The damage levels of samples were characterized by Rutherford backscattering with channeling (RBS/C) using a 2 MeV He ion beam.

RESULTS: The water temperature in the reactor tank was typically 45 - 50 °C during operation. The samples in the Al capsule were heated by nuclear reactions such as gamma-ray absorption. However, the sample temperature of the core irradiation facility cannot be directly measured during reactor operation. We estimated the sample temperature by solving a partial differential equation describing the heat flow inside the Al capsule. Assuming that the water temperature of the reactor core is 50 °C, the temperature increase inside the irradiation capsule was calculated for three different nuclear heating values (0.24, 0.36, 0.49 W/g). Even in the case of the highest nuclear heating (0.49 W/g), the temperature was below 90 °C. Since the thermal annealing rate for heavily damaged Si was nearly constant around 90 °C, we thermally annealed the control sample at 90 °C.

Figure 1 shows the RBS/C spectra of the samples after neutron irradiation and thermal annealing. A damage peak was formed near the end of range for 200 keV Si⁺. The damage peak of the thermally annealed sample was slightly lower than the peak of the as-implanted sample. On the other hand, the damage peak of the

neutron-irradiated sample was significantly lower than the peak of the thermally annealed sample. This result indicates that the neutron irradiation enhanced the annealing (recovery) of irradiation damage formed by the Si ion implantation. Although neutron irradiation slightly increases the aligned backscattering yield in the crystalline Si without ion implantation, the annealing effect of neutron irradiation was stronger than the damaging effect. The annealing efficiencies of the neutron-enhanced annealing in our previous study at 400 °C and this study at 90 °C [1, 2] were compared with the annealing efficiencies of ion beam annealing previously reported from other groups. The difference in efficiency between neutron-enhanced and ion-beam annealing processes was within one order of magnitude. It suggested that a similar mechanism may be at work for both annealing processes.

In summary, the effect of neutron irradiation on ion-implantation induced damage in Si was investigated using the core irradiation facility of KUR. The enhancement of annealing under neutron irradiation was clearly indicated by RBS/C spectra.

ACKNOWLEDGMENT: We would like to thank K. Yasuda and R. Ishigami of the Wakasa Wan Energy Research Center and colleagues of AIST for their assistance on this study.

REFERENCES:

- [1] A. Kinomura, A. Chayahara, Y. Mokuno, N. Tsubouchi, Y. Horino, T. Yoshiie, Y. Hayashi, Q. Xu, Y. Ito, R. Ishigami and K. Yasuda, Appl. Phys. Lett. 88 (2006) 241921.
- [2] A. Kinomura, T. Yoshiie, A. Chayahara, Y. Mokuno, N. Tsubouchi, Y. Horino, Q. Xu, K. Sato, K. Yasuda, and R. Ishigami, Nucl. Instrum. Methods Phys. Res. B (accepted for publication).

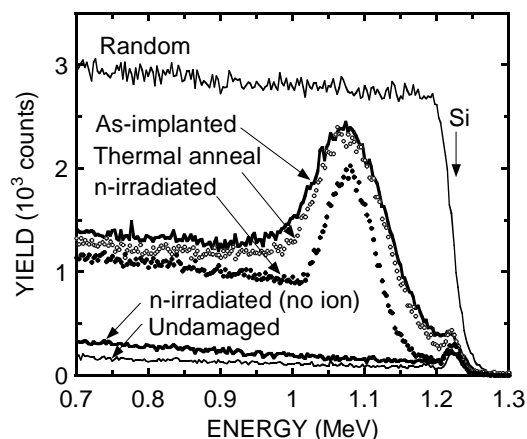


Fig. 1 RBS/C spectra of the samples after neutron irradiation (open circles) and thermal annealing (closed circles).

T. Awata, K. Nakashima and Q. Xu¹

Department of Physics, Naruto University of Education
¹Research Reactor Institute, Kyoto University

INTRODUCTION: Natural calcite irradiated by gamma rays has thermoluminescence (TL) and especially orange emission peak at 620nm which may be originated from impurity of Mn²⁺ [1]. Natural calcite also shows visible fluorescences when exposed to ultraviolet light, and that emission color depends on kinds of element impurities [2]. To clear the optical properties of natural calcite, we have measured TL and photoluminescence (PL) of natural calcite and also done impurity analysis using ICP-AES (Inductively Coupled Plasma Atomic Emission Spectroscopy).

EXPERIMENTS: The samples were natural pink calcite in Mexico and China. These samples were irradiated ⁶⁰Co gamma rays for 1h (about 20kGy) at 77K. TL spectra were measured by a photo-spectrometer (Princeton Instrument Spectra Pro 300i) with a temperature controlled system. PL spectra have been taken using PL-84 (Seishin, SOEX1702/04, R928) with He-Cd laser (Kinmon 325nm). ICP-AES (iCAP6300Duo, Thermo Fisher) was also performed to measure impurity elements concentration of calcite.

RESULTS and DISCUSSION: Figure 1 shows the TL spectra of Mexico and China calcite which are measured 93K to 413K with heating speed at 0.32K /sec. Both spectrum looks like almost same, there is one peak at 620nm. From ICP-AES results, Mexico calcite has impurities (ppm) of Fe (0.083), Mn (9.2), Pb (0.13) and Pr (1.6).

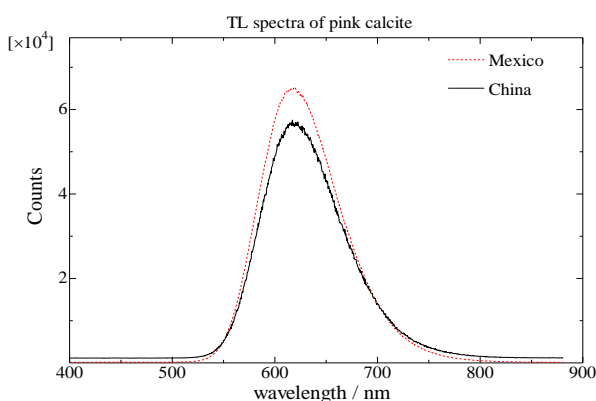


Fig. 1 TL spectrum of pink calcite in Mexico irradiated by gamma rays.

China calcite has impurities (ppm) of Fe (292), Pb (0.15), and Pr (1.5). Emission peak at 620nm with both spectrum may be related to impurity of Mn [1, 3], but cannot be detected in China sample. It might be occurred 620nm emission nevertheless very small amount of Mn exist in China calcite. Figure 2 showed the PL spectra of Mexico and China calcite irradiated by 325nm He-Cd laser at room temperature. In this spectra, there are two peaks at 560nm and 750nm in Mexico sample, there peaks at 495nm, 560nm and 750nm in China sample, respectively. A. Sidike et. al. [2] reported PL peak at 487nm was related to impurity of Pb. Photoluminescence data reference [4] reported that emission peak at 560nm for defect center. From these results, peak at 495nm on China only may be origin of Pb activate, 560nm peak on both related to defect center, intrinsically. Other peaks cannot be assigned now.

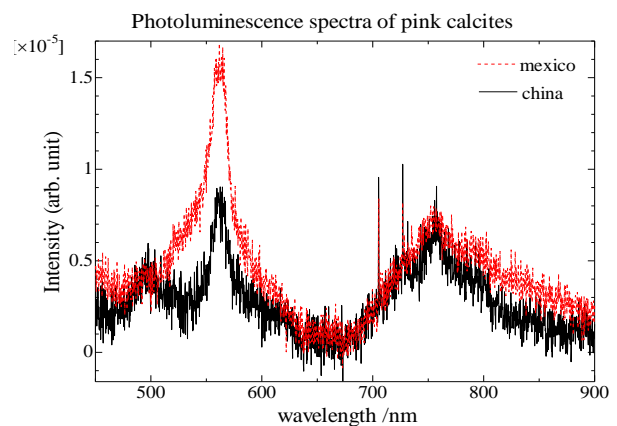


Fig.2 PL spectra of pink calcite in Mexico and in China.

ACKNOWLEDGEMENT: We would like to thank Professor S. Fukutani (KUR) for ICP-AES experiment on this study.

REFERENCES:

- [1] W. L. Medlin, *J. Opt. Soc. Am.* **53**(1963) 1276.
- [2] A. Sidike, X. M. Wang, A. Sawuti, H. -J. Zhu, I. Kusachi and N. Yamashita, *Phys. Chem. Minerals* **33** (2006) 559.
- [3] V. Ponnusamy, V. Ramasamy, M. Dheenathayalu, et al., *Nucl. Instr. and Meth. B* **217** (2004) 611.
- [4] Colin M. MacRae and Nicholas C. Wilson, *Microsc. Microanal.* **14** (2008) 184.

M. Akiyoshi, T. Yoshiie¹, Q. Xu¹ and K. Sato¹

Faculty of Engineering, Kyoto University

¹Research Reactor Institute, Kyoto University

INTRODUCTION:

It is well known that neutron-irradiated ceramics showed significant degradation in thermal diffusivity unlike metals, while thermal diffusivity during the irradiation is still not estimated. To resolve this problem, kinetic analysis is required where most important information is the behavior of point defects. Electron irradiation is the best choice to induce simple Frenkel pairs.

EXPERIMENTS:

In the previous work, 30MeV electron accelerator KURRI-Linac is used to induce point-defects in bulk specimens of typical structural ceramics to $1.5 \times 10^{24} \text{e/m}^2$ which correspond to 0.01dpa. The irradiation was performed in the water-cooled specimen holder at around 80°C. Specimens were piled between Cu heat sinks and the heat sink was put in the water chamber (Fig.1).

In addition, a new irradiation system was constructed to achieve an irradiation at around 400°C where interstitial atoms have enough mobility to migrate. In early works, several attempts to achieve such condition were made with cylindrical water jacket and Cu sleeve. All these attempts were end in failure because of a lack of thermal diffusion vertical to the beam.

Therefore, a specimen settled in Cu specimen-holder is piled between Cu heat spreaders and graphite seats. Usually, a graphite seat spreads heat well horizontally, but the graphite seat in this system is 'Vertical-Graphite' (produced by Wide work for thermal conductor on CPU) of which thermal conductivity vertical to the seat is $90 \text{W/m} \cdot \text{K}$. The piled Cu spreaders and specimen holders are tighten with Ti screws and nuts to avoid radio activation. This pile is put between Al square tubes with the vertical-graphite seats (Fig.2). All specimens and Cu plates are coated by BN spray to avoid surficial oxidation. In addition, a Cu aperture was put in front of the specimen pile to trim down the beam irradiated on out side of the specimen that heats the pile wastefully (Fig.3).

RESULTS:

Figure4 shows temperatures of test-specimen to measure the temperature at the center of specimen. Test specimens were made from soda-lime glass and Al $\phi 10 \times 0.5 \text{mm}$ disk and a slit was graven to mount a thermo couple with alumina cement. Several steps before 1000sec represent the frequency of the beam pulse. The beam condition was Acc. Energy: 32MeV, Pulse length $4 \mu\text{s}$, Peak current: 550mA. The frequency was once increased to 100Hz, but the glass specimen showed a trend of over heating compared with Al specimen, so the frequency was settled down to 80Hz. Even at that frequency,

the total beam energy was 5.8kW in several cm^2 that can compare with the heat flux on divertor in the fusion reactor ITER planed with 10MW/m^2 . This irradiation system got over this high heat flux and achieved reliable irradiation at around 400°C.

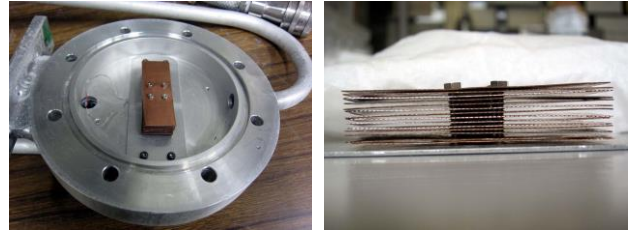


Fig.1 Water chamber and a heat sink for electron irradiation below 100°C used in the previous works.

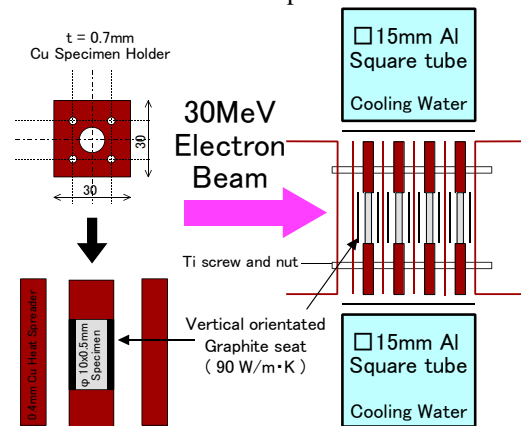


Fig.2 A schematic illustration of the new indirect water cooling irradiation system used at around 400°C.

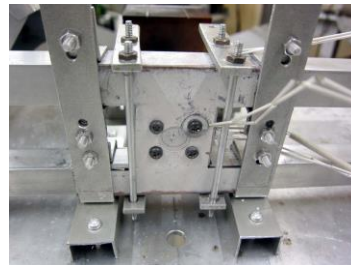


Fig.3 A photograph of the new irradiation system taken from the backside.

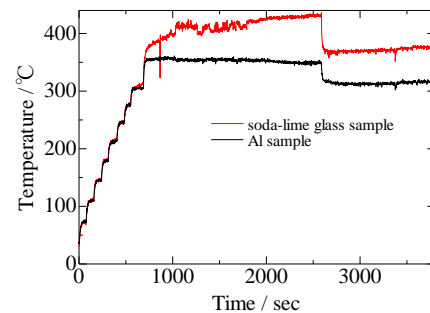


Fig.4 Temperature of the test-specimens with a gradual beam heating

Y. Nagai, K. Inoue, T. Toyama, Y. Shimizu, H. Takami-zawa, S. Wakabayashi, H. Takahama, K. Sato¹, T. Yoshie¹ and Q. Xu¹

*Institute for Materials Research, Tohoku University,
¹Research Reactor Institute, Kyoto University*

INTRODUCTION: The embrittlement of the light water reactor pressure vessel (RPV) steels due to long-term in-service exposure to neutron irradiation is one of the topical issues in the field of nuclear industry. Therefore, the mechanism of the embrittlement should be deeply understood. The ultrafine precipitation of Cu impurities contained in old RPV enhanced by the neutron irradiation and the irradiation induced defect clusters are considered to be the main origins of the embrittlement of RPV.

Positron annihilation spectroscopy is a powerful tool for detecting the ultrafine Cu precipitates in Fe and vacancy-type defects in metals sensitively. We are developing a new positron annihilation apparatus, called positron age-momentum correlation (AMOC), to study the correlation between the formation of the Cu precipitates and the defect clusters induced by neutron irradiation. For this purpose, an intense positron source is required to achieve higher count rates because typically it takes more than one week for one spectrum by the conventional AMOC system of 3 γ -rays coincidence.

In this study, a new positron beam facility is constructed at the Kyoto University Research Reactor (KUR), which is the first reactor based positron beam in Japan[1]. Separately, a new AMOC system using an avalanche photodiode is also developed.

EXPERIMENTS and RESULTS: An in-pile positron source was installed at the B-1 hole (20 cm in diameter) in KUR. The thermal neutron flux and the γ -ray flux at the positron source position are about 1.5×10^{12} n/cm² and 10^5 Gy/h, respectively, at 5 MW. A W converter of 0.2 mm thickness and W moderators with a Cd shroud are used to obtain slow positrons. In addition to the γ -rays from the reactor core, high energy γ -rays are generated by the $^{113}\text{Cd}(n, \gamma)^{114}\text{Cd}$ reaction. In the present study, a 1-mm-thickness Cd cap covered by an Al plate is used. The main modifications of the converter / moderator assembly were as follows: (i) 25 μm -thick W foils of sizes $\phi 50 \text{ mm} \times 5 \text{ mm}$ were set in a lattice. (ii) two sets of lattices were used. (iii) W converter, W moderator lattices and electric lenses were electrically isolated from each other (as shown in Fig 1). The moderators were annealed after the W strips were set in lattices. When annealing, they were encased in covered boxes of 50 μm -thick W foil and the boxes were irradiated on the covering lids with electron beam welder at KEK in Tsukuba [2]. The annealing temperature was elevated to approximately 2400°C. The vacuum of the welder chamber was about

10^{-5} torr. The slow positrons emitted from the moderator were subsequently accelerated up to 30 eV and confined magnetic fields of several mT. In order to eliminate the background of fast neutrons and γ -rays from the reactor core, the slow positron beam passes two bends in shields consisting of polyethylene, concrete and lead blocks. After passing the bends, the slow positrons are transported to sample chamber at an energy up to 30 keV. Then beam buncher is introduced for the production of pulsed positron beam, which is required for measuring of positron lifetime spectroscopy.

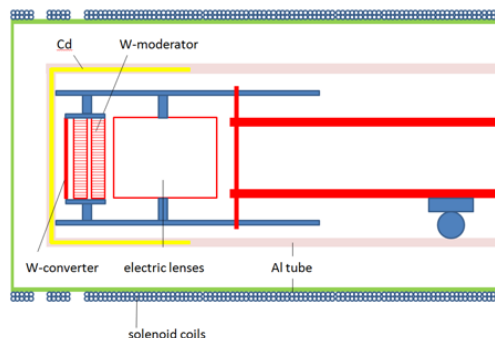


Fig. 1. A schematic diagram of the in-pile positron source at KUR [1].

Figure 2 shows a schematic diagram of the developed AMOC system, which acquires an avalanche signal for the time of positron creation, and two annihilation γ -rays of 511 keV, one used for the time of positron annihilation and the other for measuring the momentum of e^+e^- pair. Wave shapes from an avalanche photodiode, a scintillation detector and a high-purity Ge detector are directly recorded in the digital oscilloscope.

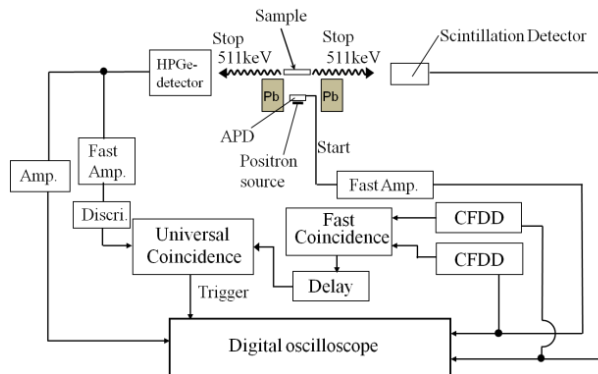


Fig. 2. A schematic diagram of the new AMOC system

The developed KUR positron beam system produced the beam intensity of about 10^6 e⁺/s at 1 MW. The developed AMOC system will be soon applied for the developed KUR positron beam system.

REFERENCES:

- [1] Q Xu *et al*, J. Phys. Conf. Ser. **505** (2014) 012030.
 [2] K Wada *et al*, Eur. Phys. J. D **66** (2012) 37.

F. Hori, K. Ishii, T. Ishiyama, A. Iwase, Y. Yokoyama¹,
Q. Xu² and K. Sato²

Dept. of Mater. Sci., Osaka Prefecture University

²*Institute of Materials Research, Tohoku University*

¹*Research Reactor Institute, Kyoto University*

INTRODUCTION: So far, we have reported that effects of free volume and mechanical properties on the bulk amorphous alloys depend upon the irradiation spaces [1,2]. Also change in free volume by the irradiation strongly reflects various properties such as hardness and ductility of bulk amorphous alloys. Essentially, the amorphous alloys have no long-range atomic periodicity with excess open volume, since liquid state is quenched by more than 10^2 K/s cooling from liquid phase to room temperature. Therefore, as quenched amorphous is not ideal glass state but includes excess open volume. It is known that annealing procedure leads ideal glass state, which is annealed out excess open volume but remains free volume. Then we performed electron irradiation for pre-annealed ZrCuAl bulk amorphous alloy, in order to understand the effects of excess open volume on the radiation damage in bulk amorphous alloy. Before and after irradiation, we have examined X-ray diffraction, differential scanning calorimetry (DSC) and positron annihilation.

EXPERIMENTS: Zr₅₀Cu₄₀Al₁₀ bulk metallic glass with 8 mm in diameter and 60 mm in length was prepared by a tilt casting technique. For positron annihilation measurements, alloy sample was cut into the size of about 0.5 mm thickness disk. Some of these quenched samples were annealed for 5 hours at 673 K, which is below glass transition temperature T_g . 8 MeV electron irradiations with total doses from 2.0×10^{17} to 2×10^{18} e/cm² was performed for these alloys at 300 K by LINAC at Research Reactor Institute, Kyoto University. During irradiation, samples were cooled in water flow path. Irradiated samples were examined by X-ray diffraction, positron annihilation lifetime and coincidence Doppler broadening measurements at room temperature. The positron annihilation lifetime spectra consist of more than 1.0×10^6 counts. The positron lifetime spectra were analyzed by the POSITRONFIT program.

RESULTS: The mean positron lifetime τ of as-quenched and pre-annealed samples are 166 and 157 psec, respectively. Before irradiation, positron lifetime decreases showing the shrinkage of free volume by pre-annealing. Figure 1 shows the change in positron annihilation lifetime by electron irradiation as a function of irradiation fluence for Zr₅₀Cu₄₀Al₁₀ bulk metallic glasses. Solid line and broken lines show that positron lifetime for as quenched and annealed samples respectively. The increasing trend of positron lifetime with increase of irradiation fluence is clearly different between as-quenched and structural relaxed samples. In the case of as-quenched sample, the positron lifetime increases gradually at about 5×10^{17} e/cm² irradiation, but in case of pre-annealed sample the positron lifetime increases at low fluence of electron irradiation and its value is almost constant. We found that radiation effects for bulk amorphous alloys are strongly depend on the initial state before irradiation [3].

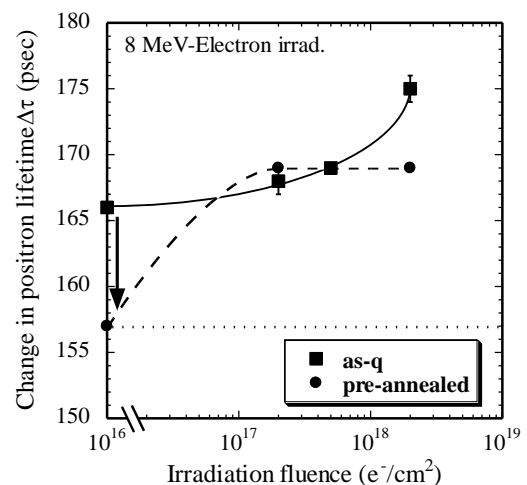


Fig. 1 Change in positron lifetime for as-quenched and pre-annealed ZrCuAl bulk glassy alloy with 8 MeV electron irradiation.

REFERENCES

- [1] N.Onodera, A.Ishii, Y.Fukumoto, A.Iwase, Y.Yokoyama, and F.Hori, Nucl. Inst. & Meth. B. 282 (2012) 1
- [2] F.Hori, N.Onodera, A.Ishii, Y.Fukumoto, A.Iwase, A.Kawasuso, A.Yabuuchi, M.Maekawa and Y.Yokoyama, J. Phys.: Conf. 262 (2011) 012025
- [3] N.Onodera, A.Ishii, A.Iwase, Y.Yokoyama, K.Sato, Q.Xu, T.Yoshiie and F.Hori, J. of Phys. Conf. Ser. 443 (2013) 012022

PR9-8 Positron Annihilation Study on Fe-40Cr Alloy after Electron Irradiation

T. Onitsuka, K. Fukumoto, K. Sato¹ and Q. Xu¹

Research Institute of Nuclear Engineering, Fukui University

¹Research Reactor Institute, Kyoto University

INTRODUCTION: High-chromium (9-12%Cr) Ferritic/martensitic steels are attractive candidate material for various nuclear energy systems because of their excellent thermal properties, higher swelling resistance and lower activation compared with conventional austenitic stainless steels. The high-chromium steel as also been considered for both in-core and out-of-core applications of fast breeder reactors, and for the first wall and blanket structures of fusion systems, where irradiation induced degradation is expected to be the critical issues for reactor operation [1]. The general progressive change in microstructure with irradiation dose and temperature involves dislocation loops and radiation-induced precipitate can degrade material properties. Precipitates formed in the 9-12%Cr steels during irradiation include α' , G-phase, M_6C , and χ -phase. In this present study, the authors focused on a precipitation response for formation of α' -phase in Fe-Cr binary model alloy subjected to electron irradiation, in order to examine fundamental aspects of radiation effects on α' -phase precipitate development in iron-chromium alloys. Positron annihilation measurement technique was used to study the behavior of microstructural evolution due to irradiation-induced defects and the formation of α' -phase simultaneously. Because the phase decomposition into Fe-rich (α) and Cr-rich (α') phases will co-occur in Fe-Cr alloy, the formation of α' -phase precipitate can be detected by positron annihilation coincidence Doppler broadening (CDB) technique owing to lesser positron affinity for Cr than Fe.

EXPERIMENTS: Simple binary Fe-40Cr alloy was made by arc melting under argon atmosphere in a water-cooled copper hearth. All the ingots were melted and inverted three times in order to promote chemical homogeneities. The obtained ingot was conducted with solution heat treatment at 1077 °C for 2 h followed by water quenching, and then, machined to the dimensions of 10mm × 10 mm × 0.5 mm. All specimens were lapped followed by chemo-mechanical polish using a suspension of colloidal silica (0.05 μ m) to remove surface damage from previous steps. 9 MeV electrons irradiated at 100 °C in KURRI-LINAC. The irradiation dose and displacement damage ranges were 3.0×10^{17} - 2.0×10^{18} e/cm² and 0.04-0.3 mdpa. After irradiation, positron annihilation CDB measurement was performed at the hot laboratory

of KURRI. The conventional analysis from radiation annihilation line-shape parameter S and W was used to characterize irradiation induced Fe/Cr decomposition behavior.

RESULTS: The S-W plots obtained from positron CDB measurements for Fe-40Cr alloy before (WQ) and after (0.04-0.3 mdpa) irradiation is shown in Fig. 1. In general, positron trapping in vacancies results in an increase (decrease) in S- (W-) parameter, since annihilation with low-momentum valence electrons increased at vacancies. A high concentration of defects, or an increase in the mean size of defects leads to a larger contribution of annihilations from low momentum electrons because positrons are trapped at defects. This is reflected in CDB measurements by an increase in S-parameter and a decrease in W-parameter as irradiation dose is increased. However a rapid and significant decrease of S-parameter comparable with a rapid and significant increase of W-parameter respectively observed between 0.1 mdpa and 0.2 mdpa. This behavior of S- and W- parameters means an abrupt change at the positron annihilation site. Further experiments are ongoing.

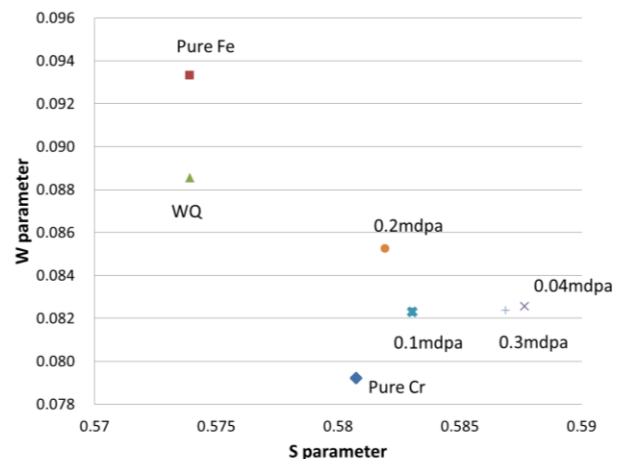


Fig. 1 S-W plots obtained from positron CDB measurements of Fe-40Cr alloy before (WQ) and after electron irradiation at 100 °C to 0.04, 0.1, 0.2, 0.3 mdpa, respectively. Pure Fe and Pure Cr are plotted for comparison.

REFERENCES:

[1] R. L. Klueh, International Materials Reviews, **50** (2005) 287-310.

I. Mukouda, K. Yamakawa¹, Q. Xu² and K. Sato²

Hiroshima International University

¹*Faculty of Engineering, Ehime University*

²*Research Reactor Institute, Kyoto University*

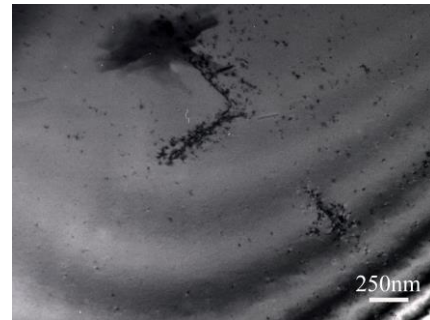
INTRODUCTION: Copper and nickel are used as typical FCC metals in radiation damage studies. Many studies have been carried out and reviewed by Singh and Zinkle [1]. They concluded that there is a lack of information on the microstructure of copper and nickel irradiated to below 10^{-2} dpa at 100 to 300°C [1]. Zinkle and Snead carried out fission neutron irradiation at 230°C to damage levels between 10^{-2} and 10^{-1} dpa [2]. They concluded that a high density of small SFT and dislocation loops was observed in copper and nickel, and small voids were observed in irradiated copper. Recently Shimomura and Mukouda carried out fission neutron irradiation of copper at 200 and 300°C at a similar range of dose, we reported dose dependence of voids and SFTs previously. The present work is carried out to examine the evolution of vacancy clusters and voids in neutron-irradiated copper of transient regime at elevated temperatures. To obtain precise results, the irradiation was carried out at the temperature controlled irradiation facility in the KUR.

EXPERIMENTAL PROCEDURES: The specimens used in this study were pure copper and nickel. Specimens were cold-rolled to 0.05 mm and punched out to disks of 3mm in diameter, and annealed in vacuum. Neutron irradiation was carried out in the temperature controlled capsule at KUR reactor in SSS at 1MW. The specimen temperature was kept at 300°C or 200°C during irradiation. After radiation cooling, specimens were electro-polished and using JEOL-2010 TEM at an accelerating voltage of 200kV. Void images were observed by bright field technique of off-Bragg diffraction condition (void contrast) and weak beam dark field (WBDF) image.

RESULTS AND DISCUSSIONS: Figure 1 shows TEM observation of neutron- irradiated copper at 200°C, 2.9×10^{17} n/cm², by bright field image. Pre-existing dislocations were observed in this to be decorated by interstitial clusters and small stacking fault tetrahedron (SFT). Fig. 2 and 3 shows TEM observation of same specimen by dark field image. SFT and interstitial clusters were observed. Number density of clusters were increased gradually. The number density of voids and point defect clusters were smaller than irradiation at 5MW 200°C specimen [3]. Fast neutron flux was 1.7×10^{13} at 5MW, 3.4×10^{12} n/cm²s. Another irradiation conditions are progressing now.

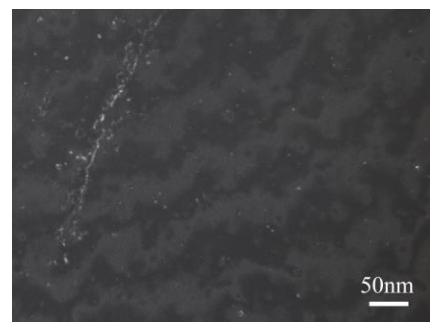
REFERENCES

- [1] B. N. Singh and S. J. Zinkle, *J. Nucl. Mater.*, **206**, (1993) 212.
 [2] S. J. Zinkle and L. L. Snead, *J. Nucl. Mater.*, **225**, (1995) 123.
 [3] I. Mukouda and Y. Shimomura, *Mat. Res. Soc. Symp. Proc.*, **650** (2001) R3.11.1-R3.11.6.



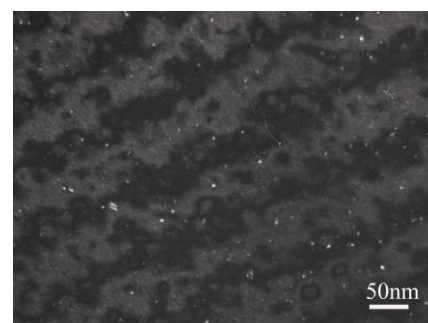
KUR 1MW 200°C 23h

Fig. 1. TEM observation of neutron- irradiated copper at 200°C, 2.9×10^{17} n/cm², by bright field image.



KUR 1MW 200°C 23h

Fig. 2. TEM observation of neutron- irradiated copper at 200°C, 2.9×10^{17} n/cm², by dark field image, (g,5g) g=200.



KUR 1MW 200°C 23h

Fig. 3. TEM observation of neutron- irradiated copper at 200°C, 5.7×10^{17} n/cm², by dark field image, (g,5g) g=200.

R. Kasada, K. Sato¹ and Q. Xu¹

Institute of Advanced Energy, Kyoto University

¹*Research Reactor Institute, Kyoto University*

INTRODUCTION: Ferritic steels containing Cr are expected to be used for the first-wall component of the fusion reactors as well as the fuel pin cladding of the Generation IV nuclear fission systems [1]. However, high-Cr steels may suffer from thermal aging embrittlement, which is well-known 475 °C embrittlement. This is mainly due to hardening phenomenon through the phase separation of Fe and Cr as shown in the phase diagram. In the previous study [2], we applied a positron annihilation spectrometry to detect the phase separation in the Fe-Cr alloys under “the Strategic Promotion Program for Basic Nuclear Research by the Ministry of Education, Culture, Sports, Science and Technology of Japan”.

The present collaborative research has investigate the neutron irradiation effect on the phase separation of Fe-Cr ferritic alloys and the following hardening behavior. In the FY2013 we have obtained the result of irradiation hardening on the Fe-Cr binary alloys after the neutron irradiation in KUR.

Experimental Procedure: Materials used in the present study are $Fe_{1-x}Cr_x$ binary alloys. Neutron irradiation on these materials was carried out at 300 °C up to 199 h in KUR. The displacement damage is 2.1×10^{-3} dpa (5.1×10^{18} n/cm²). Micro-Vickers hardness was measured with a load of 0.1 kgf at the ambient temperature in the hot laboratory of KURRI.

Results and Discussions: The Cr-dependence of irradiation hardening of Fe-Cr alloys after the KUR irradiation is shown in Fig. 1. It is noticed that pure Fe ($x=0$) shows no significant change in the hardness but pure Cr ($x=1$)

shows irradiation hardening. This difference is possibly due to the production rate of irradiation-induced clusters (interstitial type and/or vacancy type) between them. Preliminary results of positron annihilation lifetime spectrometry shows formation of vacancy clusters in Pure Cr after the neutron irradiation. In addition, the amount of irradiation hardening of the Fe-Cr alloys is not a linear function of the Cr concentration. Previous study on the thermal aging effect on the hardening of Fe-Cr alloys suggests that such nonlinear behavior is due to the phase separation of Fe-Cr binary alloys. Further experiments on the microstructural development in the irradiated Fe-Cr alloys are now going.

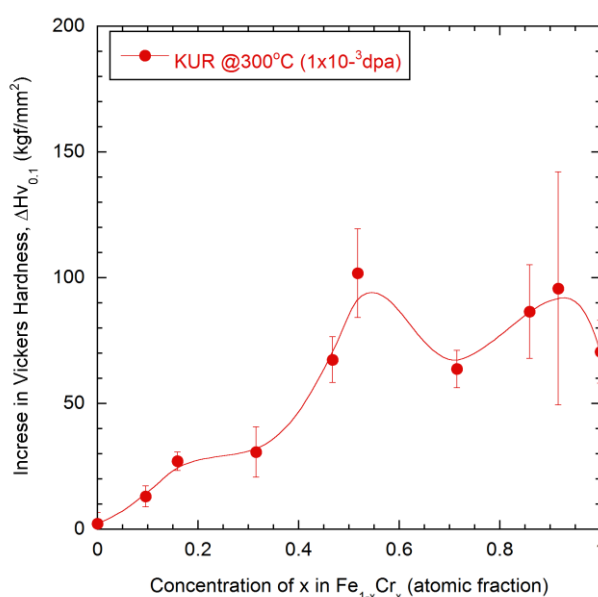


Fig. 1 Cr-dependence of irradiation hardening of Fe-Cr alloys after the KUR irradiation.

REFERENCES:

- [1] A. Kimura, *et al.*, J. Nucl. Sci. Technol., **44** (2007) 323-328.
- [2] R. Kasada and K. Sato, to be submitted.

H. Tsuchida, H. Tsutsumi¹, S. Mizuno¹, A. Itoh¹, K. Sato², T. Yoshiie² and Q. Xu²

Quantum Science and Engineering Center, Kyoto University

¹*Department of Nuclear Engineering, Kyoto University*

²*Research Reactor Institute, Kyoto University*

INTRODUCTION: Effects of neutron irradiation on nuclear reactor materials are of technical importance for evaluation of age-related deterioration of the materials. Neutron irradiation induces radiation damage (defect production) as well as produces nuclear reaction products, such as hydrogen atoms or helium atoms. These products cause a change in materials properties, for instance a loss of ductility of materials arising from hydrogen embrittlement.

Nanocrystalline (NC) materials with grain size of less than a few tens micrometers are known to have high resistance to radiation damage effects, because the grain boundaries act as effective sinks that absorb radiation-induced defects. In addition, the grain boundaries may absorb nuclear reaction products, such as hydrogen atoms or helium atoms. Thus, it is expected that NC materials have two different properties on response to neutron irradiation.

To understand the mechanism of hydrogen embrittlement for NC materials, we study experimentally hydrogen trapping sites at grain boundaries in NC materials irradiated with neutrons. We analyzed microstructures of the grain boundaries at which hydrogen atoms were absorbed, by using positron annihilation lifetime spectroscopy.

EXPERIMENTS: Specimens were nanocrystalline Ni having the average grain size of 30 nm. The specimens were irradiated by neutrons from KUR up to 1.8×10^{-3} dpa. For specimens after irradiation, deuterium (as an alternative atom of a hydrogen atom) was loaded into the specimens by charging with highly pressured (3 MPa) deuterium gas at 373 K for 7 hours. The deuterium-absorbed specimens were kept at liquid nitrogen temperature of 77 K for prevention of the release of deuterium atoms. To investigate hydrogen trapping sites in the specimens, we performed measurements of positron annihilation lifetime spectroscopy (PALS) at different temperatures ranging from 77 K to 300 K.

RESULTS: Figures 1 and 2 show experimental results for temperature dependence of positron lifetime for NC Ni irradiated by neutrons at 1.8×10^{-3} dpa. Positron lifetime spectra were analyzed by two components τ_1 and τ_2 , where the τ_1 is attributed to positron trapping at the free volumes in the crystalline interfaces and the τ_2 corresponds to the free volumes at the intersections of two or

three crystallites interfaces. We investigate a change in the τ_1 or the τ_2 component for the irradiated specimens before and after deuterium loading. It was found that for the τ_1 no change was observed. In contrast, the value of τ_2 reduces from 414 ps (before loading of deuterium) to 350 ps (after loading). This reduction indicates deuterium trapping into the grain boundaries. According to the calculation by Shivachev *et al.* [1], the observed reduction suggests that the number of trapped deuterium atoms trapped into the free volumes at the intersections is 4-6. It was concluded that the grain boundaries of intersections are damaged by irradiations, and serve as a trap site of nuclear reaction products.

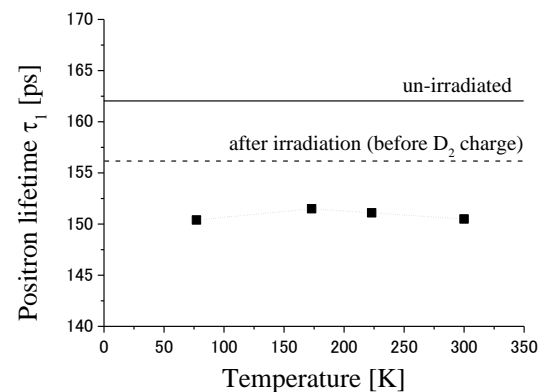


Fig.1. Annealing behavior of the τ_1 component for deuterium-absorbed specimens after neutron irradiation at 1.8×10^{-3} dpa.

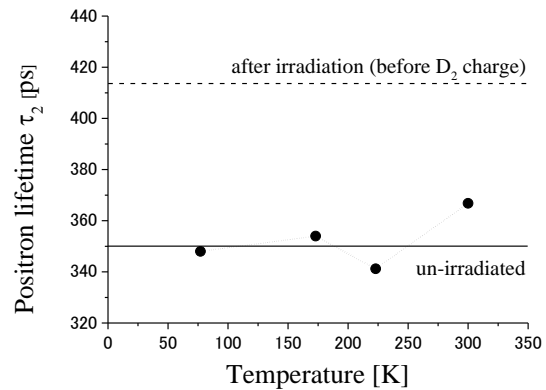


Fig. 2. Annealing behavior of the τ_2 component for deuterium-absorbed specimens after neutron irradiation at 1.8×10^{-3} dpa.

REFERENCES:

[1] B. L. Shivachev *et al.*, *J. Nucl. Mater.*, **306** (2002) 105-111

K. Sato, Q. Xu, X.Z. Cao¹, P. Zhang¹, B.Y. Wang¹,
T. Yoshiie, H. Watanabe² and N. Yoshida²

Research Reactor Institute, Kyoto University

¹ Institute of High Energy Physics, Chinese Academy of Sciences

² Research Institute for Applied Mechanics, Kyushu University

INTRODUCTION: Interest in the behavior of hydrogen (H) and its isotopes in solids has increased with advances in fusion reactor technology. Plasma-facing materials (PFMs) in fusion reactors suffer displacement damage caused by high-energy neutrons, and surface damage caused by hydrogen and helium from the plasma. Important criteria for PFM selection are a high melting point, high thermal conductivity, and low sputtering erosion. Metallic materials such as tungsten (W) and molybdenum are potential candidates for PFMs, according to the results of recent studies. Generally, W has very low solubility for hydrogen isotopes, but intrinsic and radiation-induced defects can retain a significant amount of H. Therefore, the inventory of the hydrogen isotope tritium (T) in PFMs is an important issue for the International Thermonuclear Experimental Reactor [1-3]. The positron annihilation technique is a very powerful tool in the study of fundamental microstructural features, such as small vacancy-type defects, of localized sites in condensed matter [4]. In the present study, defect formation in ion-irradiated W and the interaction between defects and deuterium (D) instead of T were investigated by positron annihilation spectroscopy.

EXPERIMENTS: Samples were prepared from polycrystalline W (99.95 wt%) obtained from Allied Material Corporation. A 0.2-mm-thick W plate was cut into 10×10 mm² samples, and mechanically polished to a mirror-like finish. The samples were then annealed at 1773 K for 1 h in vacuum with a background pressure of 1×10⁻⁴ Pa. After electropolishing in 4% aqueous NaOH solution at 15 V, the samples were irradiated with 2.4 MeV Cu²⁺ ions at room temperature using a tandem-type accelerator at Kyushu University, Japan. The damage peak was about 400 nm from the irradiated surface, according to calculations using the SRIM code. The damage rate was 2.5×10⁻⁴ dpa/s, and the total damage was 0.3 dpa at the peak position. The Cu ion fluence was 1.6×10¹⁸ ions/m². D implantation was subsequently carried out in samples using a mono-energetic D₂⁺ ion beam at room temperature. To avoid displacement damage, implantation was performed at 1 keV (500 eV/D⁺). The implanted D ions lay 0-20 nm from the incident surface, and the D distribution peak was roughly 8 nm from the surface. D atoms

diffused freely in the W matrix until they were trapped by defects induced by Cu ion irradiation. The diffusion length of D atoms was larger than their range. The nominal D dose was 1×10²¹ D/m². In order to investigate the irradiation depth dependence of the microstructural evolution, the Doppler broadening of annihilation radiation measurements were performed using a mono-energetic positron beam apparatus at the Institute of High Energy Physics, Chinese Academy of Sciences. The positron implantation profiles broadened gradually with increasing beam energy. At E=20 keV, most positrons are stopped within the damaged region formed by 2.4 MeV Cu ions.

RESULTS: We introduce two parameters, *S* and *W*, defined as the ratio of the low-momentum ($|P_L| < 1.5 \times 10^{-3} m_0 c$) and high-momentum ($5 \times 10^{-3} m_0 c < |P_L| < 13 \times 10^{-3} m_0 c$) regions in the Doppler broadening spectrum to the total region, respectively, where m_0 is the electron rest mass and c is the velocity of light. *S* parameter represents the smaller Doppler shift resulting from the annihilation of valence electrons, and *W* parameter comes from the annihilation at core electrons, which is used to estimate the interaction with D atoms around positrons when they are annihilated. *S* parameter decreased with increasing positron energy in unirradiated W. The high *S* parameter at low incident positron energies is due to positron diffusion to the surface and consequent production of ortho-positronium. The surface effects decrease with increasing positron energy. Although the variation in *S* parameter with positron energy in ion-irradiated W was the same, *S* parameter was higher in ion-irradiated W than in unirradiated W. It has been reported that vacancy clusters were formed as a result of ion irradiation. Thus, a high *S* parameter indicates that vacancy-type defects were formed during ion irradiation. Compared with W before and after ion irradiation, the decrease in *S* parameter in D-implanted W with increasing positron energy slowed down when the positron energy was higher than 4 keV. *S* parameter was lower in D-implanted W than in ion-irradiated W at positron energies below 18 keV. It has been reported that trap energy of first D atom at a vacancy was 1.34 eV. In addition, Troev et al. showed that the lifetime of vacancies decreased after trapping H atoms. Thus, D atoms were trapped by vacancies produced by Cu irradiation.

REFERENCES:

- [1] V.K. Alimov *et al.*, J. Nucl. Mater. **420** (2012) 370-373.
- [2] Y. Oya *et al.*, Phys. Scr. **T145** (2011) 014050.
- [3] K. Tsukatani *et al.*, Fusion Sci. Technol. **60** (2011) 1543-1547.
- [4] A. Dupasquier *et al.*, Positron Spectroscopy of Solids (1995, IOS Press, Amsterdam).

Y. Hatano, K. Ami, K. Sato¹ and Q. Xu¹

Hydrogen Isotope Research Center, University of Toyama

¹Research Reactor Institute, Kyoto University

INTRODUCTION: Tungsten (W) is currently recognized as a primary candidate of plasma-facing material (PFM) for future fusion reactors. Therefore, various properties of W including hydrogen isotope retention have been investigated. In Japan-US Joint Research Project TITAN, the influence of neutron (n) irradiation on deuterium (D) retention in W under high-flux plasma exposure was examined. [1–2] Neutron irradiation up to 0.3 dpa (displacement per atom) at around 423 K resulted in clear increase in D retention in W, and the D concentration reached $[D]/[W] = 0.08$ at 473 K and $[D]/[W] = 0.03$ at 773 K. The large hydrogen isotope retention in irradiated W should have a strong impact on tritium inventory in vacuum vessels of fusion reactors, and hence it is necessary to clarify the trapping mechanisms and develop techniques to mitigate the irradiation effects. However, the types of defect playing dominant roles in trapping effects have not been understood. Because of cascade collisions, high energy neutrons can create various types of defects including dislocation loops, mono-vacancies and vacancy clusters. It is difficult to understand the trapping effects of each type of defect using a sample with such large variety of defect types. The goal of this study is to examine the effects of mono-vacancy on hydrogen isotope trapping in W using high-energy electron (e) beam.

Electron irradiation: Because of its small mass, high-energy electron induces only Frenkel pairs (a pair of mono-vacancy and an interstitial atom) in W and not collision cascade. At around room temperature, vacancies are immobile, whereas interstitial atoms can migrate and be annihilated at sinks or by the recombination with vacancies. Hence, the types of radiation defects being expected to be induced by electron irradiation are mono-vacancy and interstitial-type dislocation loop. There is a large difference in trapping energy of hydrogen isotopes between dislocation (0.85 eV [2]), and mono-vacancy (1.45 eV [2]), and hence hydrogen isotope atoms trapped in these two types of defects may be separated from each other by thermal desorption spectroscopy (TDS). In this study, irradiation of 8 MeV electrons were performed at around room temperature up to $\sim 10^{-3}$ dpa for two types of W samples; W-coating prepared by a vacuum plasma spray (VPS) technique on carbon/carbon-fiber composite (CFC) (400 μm thickness) and disks of bulk W annealed at 1173 K for stress-relieving (200 μm thickness). After the CFC sub-

strate was removed by mechanical polishing, the VPS-W sample was exposed to D₂ gas at 100 kPa and 673 K for 10 hours, and then TDS measurements were performed at 0.5 K s⁻¹. The irradiated bulk W will be subjected to D₂ gas exposure and TDS measurements in the near future. Non-irradiated samples were/will be also examined for comparison.

RESULTS: The D concentration in the non-irradiated VPS-W sample was $[D]/[W] = 1 \times 10^{-6}$. The electron irradiation resulted in increase in D concentration to $[D]/[W] = 3 \times 10^{-5}$. D retention increased by an order of magnitude with irradiation as low as 10^{-3} dpa. Such significant increase in D retention was ascribed to trapping by radiation defects. The TDS spectrum of D from e-irradiated VPS-W sample is shown in Fig. 1 together with that from n-irradiated W exposed to D plasma at 773 K [1]. The characteristic points of TDS spectrum from n-irradiated W are large D retention and high desorption temperature; desorption from non-irradiated sample was completed at around 900 K while that from n-irradiated sample was incomplete even at 1173 K. The spectrum of e-irradiated VPS-W sample peaked at 800 K and showed a tail to high temperature sides which indicates the presence of strong traps. The analysis with TMAP4 program [3] suggested that the peak position corresponds to the trapping energy of ~ 1.5 eV which is comparable with that of mono-vacancy [2]. The origin of the tail has not been clarified. In general, porosity and impurity content of VPS-W are higher than those of bulk W. More detailed discussion will be possible after the measurements of TDS spectrum from the e-irradiated bulk W sample.

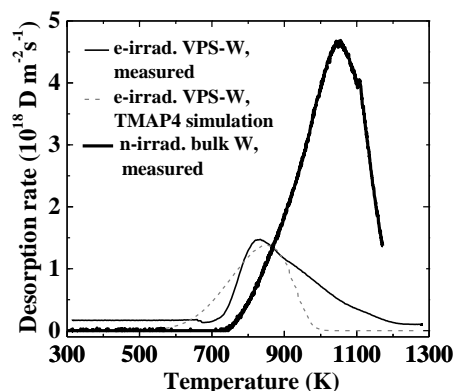


Fig. 1 TDS spectrum of D from electron-irradiated VPS-W and neutron-irradiated bulk W [1].

REFERENCES:

- [1] Y. Hatano *et al.*, Nucl. Fusion, **53** (2013) 073006.
- [2] O.V. Ogorodnikova, J. Nucl. Mater., **390–391** (2009) 651–654.
- [3] G. R. Longhurst *et al.*, TMAP4 User's Manual, EGG-FSP-10315, doi: 10.2172/7205576.

K. Shigematsu, K. Betchaku, K. Morita, K. Yokoyama,
N. Nitta and M. Taniwaki

Kochi University of Technology

INTRODUCTION: The characteristic cellular structure is formed by ion-irradiating on compound semiconductors GaSb and InSb, and an elemental semiconductor Ge [1-3]. This nanocell structure with fine dimensions is expected to be applied to nanotechnology. Our research group has made the ordered nanocell lattices using focused ion beam (FIB) [4-6]. The idea in this work is to use the thin wall partitioning cells as the tunneling barrier in Josephson junction. We will obtain Josephson junction devices by filling the cells with superconducting materials. For this application, the dimensions, especially, the thickness of the partitioning wall is important. The wall thickness must be smaller than 10 nm in the case of metal superconductors and less than that in high T_c superconductors, for this application. We chose GaSb as the material of the nanocell from the results of our past works. The wall thickness in GaSb cell structure was 5 nm which was much smaller than those in InSb and Ge. In this work, the effect of the temperature on nanocell structure during fabrication was investigated in order to obtain nanocells fit for Josephson junction.

EXPERIMENTS: The FIB apparatus used in this work was Quanta 3D 200i (FEI company) attached with a low temperature stage, in which the temperature of the sample is controlled from 80 K to 300 K. The procedure of nanocell fabrication is shown in Fig. 1.

First, we made the nanocell lattices with a 100 nm cell interval in FIB at room temperature and at 135 K and observed these structures by FE-SEM and the effect of the sample during ion irradiation. Next, more fine nanocells were fabricated at 123 K, 173K, 223K and room temperature.

RESULTS: Figure 2 shows the 100 nm nanocells fabricated at room temperature and a low temperature. Although the wall thickness was very fine (less than 10 nm) in the

sample at room temperature, the lattice regularity was disturbed. This is due to the secondary void which formed between cells. On the other hand, in the sample at 135 K, the regularity was perfect but the wall thickness was about 25 nm which was too large for Josephson junction. It is considered that the formation of the secondary voids is due to the high mobility of vacancies induced by ion irradiation and the large thickness of the wall is due to the poor mobility of the vacancies. From this, it is considered that ordered nanocell with a finer lattice interval will be obtained at room temperature and more ion doses will be necessary in order to obtain thinner wall thickness. In the experiment of obtaining finer nanocell lattice, we succeeded in fabrication of 40 nm lattices at 123 K – room temperature. Now, we are searching for the appropriate substrate temperature and cell interval for Josephson junction devices.

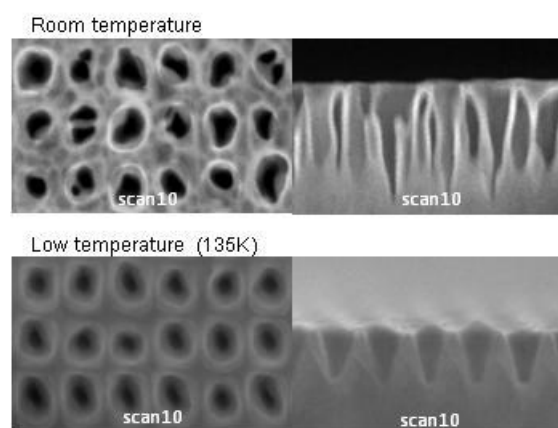


Fig 2. SEM photographs of nanocells fabricated at room temperature and 135 K.

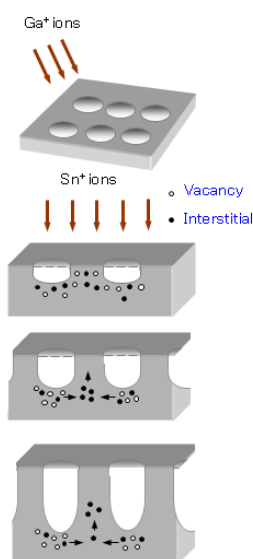


Fig 1. Nanocell fabrication procedure

REFERENCES

- [1] N. Nitta, M. Taniwaki, T. Suzuki, Y. Hayashi, Y. Satoh and T. Yoshiie: Mater. Trans. **43** (2002) 674-680
- [2] N. Nitta, M. Taniwaki, T. Suzuki, Y. Hayashi, Y. Satoh and T. Yoshiie: J. Japan Inst. Metals **64** (2000) 1141-1147
- [3] N. Nitta, M. Taniwaki, Y. Hayashi and T. Yoshiie: J. Appl. Phys. **92** (2002) 1799-1802
- [4] N. Nitta and M. Taniwaki: Nucl. Instrum. Methods B **206** (2003) 482-485.
- [5] N. Nitta, S. Morita and M. Taniwaki: Surf. Coat. Technol. **203** (2009) 2463-2467.
- [6] M. Taniwaki, S. Morita and N. Nitta: AIP Conference Proceedings Series, 20th International Conference on the Application of Accelerators in Research and Industry (CAARI 2008), (2009) pp.524-527.